Philosophical Magazine,
Vol. 85, No. 1, 1 January 2005, 45–64

Rumpling instability in thermal barrier systems under isothermal conditions in vacuum

Rahul Panat, K. Jimmy Hsia† and Joseph Oldham

Department of Theoretical and Applied Mechanics,
University of Illinois, Urbana, IL 61801, USA

[*Received 4 January 2004 and accepted in revised form 25 August 2004*]

Abstract

Bond coat (BC) surface rumpling has been identified as one of the important mechanisms that can lead to failure of thermal barrier coatings. The driving force behind rumpling—whether the stresses in the thermally grown oxide over the BC or the stresses in the BC—remains to be clarified. Also, the mass transport mechanisms in the BC leading to rumpling are not clearly identified. In the present investigation, we subjected two types of BC–superalloy systems, nickel aluminide and platinum aluminide BCs on a Ni-based superalloy, to isothermal exposure at temperatures ranging from 1150°C to 1200°C in vacuum. The results show that the nickel aluminide BC rumples at 1200°C and at 1175°C in the absence of significant oxidation. The wavelength of the rumpled surfaces was 60–100 μm, with an amplitude of 5–8 μm. The rumpling was insensitive to the initial BC surface morphology. At 1150°C, no clear rumpling was observed, but some surface undulations could be seen related to the BC grains. The platinum aluminide BC with an initially polished surface showed the formation of dome-like structures corresponding to the BC grains at 1200°C, indicating a strong influence of BC grain boundary diffusion on the BC rumpling. The above observations indicate that large-scale mass transport manifested in the form of BC rumpling can occur in the absence of a significant oxide layer. The stresses in the BC appear to be sufficient to cause the rumpling behaviour. The current rumpling results are discussed in the context of the possible mechanisms. It is concluded that various diffusive processes (grain boundary, surface and bulk diffusion) in the BC driven by the BC stresses lead to the rumpling behaviour observed in the current study.

§ 1. Introduction

Thermal barrier coatings (TBCs) have been developed to boost the performance of gas turbines, jet engines, and diesel engines (Strangman 1985, Miller 1987, Sheffler and Gupta 1988, Meier and Gupta 1994, Goward 1998, Stiger *et al*. 1999, Padture *et al*. 2002, Schulz *et al*. 2003). TBCs are multi-layered structures that help reduce the temperature of the hot components in these applications, resulting in improved efficiency, or equivalently, the component creep life in these applications. A TBC system consists of: (i) a ceramic top layer that provides the required temperature gradient, (ii) an intermediate (metallic) bond coat (BC) deposited on the base superalloy to enhance the TBC oxidation resistance and improve the adherence of the

† Author for correspondence. Email: kjhsia@uiuc.edu

Philosophical Magazine ISSN 1478–6435 print/ISSN 1478–6443 online
http://www.tandf.co.uk/journals
DOI: 10.1080/14786430412331309344

ceramic top layer, and (iii) a thermally grown oxide (TGO) that forms over the BC surface at the BC–ceramic interface and continuously evolves at high temperature.

One of the problems limiting the use of TBCs is ceramic topcoat spallation after a certain amount of thermal exposure. The topcoat spallation is quite dangerous since the local operating temperatures in the gas turbine hot sections can exceed the melting temperature of the superalloy substrate. The TBC failure problem has been investigated under isothermal, thermomechanical and cyclic thermal histories (McDonald and Hendricks 1980, Miller and Lowell 1982, Wu *et al.* 1989, Bartlett and Maschio 1995, Bose and Demasi-Marcin 1997, Wright 1998, Clarke and Shillington 1999, Bouhanek *et al.* 2000, Ibegazene-Ouali *et al.* 2000, Vaidyanathan *et al.* 2000, Ambrico *et al.* 2001, Bartsch *et al.* 2001, Baufeld *et al.* 2001, Busso *et al.* 2001, Ruud *et al.* 2001, Schulz *et al.* 2001, Tolpygo and Clarke 2001, Tolpygo *et al.* 2001, Ali *et al.* 2002, Kim *et al.* 2002, Bartsch *et al.* 2003). The TBC failure is seen to vary from system to system (Bouhanek *et al.* 2000, Ruud *et al.* 2001, Schulz *et al.* 2001, Tolpygo and Clarke 2001, Tolpygo *et al.* 2001). One of the significant indications from these studies is that the failure process is associated with instabilities occurring at the BC–ceramic interface, with the TGO in between (Wright and Evans 1999, Evans *et al.* 2001). One such instability is BC surface *rumpling*, or progressive roughening of the BC surface to characteristic wavelengths in BC–superalloy systems upon thermal cycling (Deb *et al.* 1987, Holmes and McClintock 1990, Pennefather and Boone 1995, Zhang *et al.* 1999, Tolpygo and Clarke 2000, Panat and Hsia 2004). The rumpling instability in the presence of the ceramic topcoat creates a geometric incompatibility in the form of cracks at the BC (or TGO)–ceramic interface, and contributes to TBC failure (Tolpygo and Clarke 2000, 2001, Mumm *et al.* 2001, Baufeld and Barstch 2003). This instability is shown to be suppressed under certain circumstances, e.g., when the TGO–ceramic interface remains intact (Tolpygo and Clarke 2001). The suppression of rumpling can, however, give rise to residual stresses at the BC–TGO interface and contribute to other TBC failure processes (e.g. BC–TGO separation). This necessitates a thorough understanding of the mechanisms of BC rumpling.

Several experimental (Deb *et al.* 1987, Holmes and McClintock 1990, Pennefather and Boone 1995, Zhang *et al.* 1999, Tolpygo and Clarke 2000, Panat and Hsia 2004) and theoretical (Suo 1995, He *et al.* 2000, Tolpygo and Clarke 2000, Karlsson and Evans 2001, Balint and Hutchinson 2003, Panat *et al.* 2003) studies have been carried out to address the problem of the surface rumpling of an overlay metallic coating on a metal (usually superalloy) substrate, often referred to as *bond-coat rumpling* (here we continue to use the terminology 'bond coat' even though there is no longer a ceramic topcoat in these studies). Platinum aluminide, nickel aluminide and NiCoCrAlY BCs deposited on superalloy substrates were shown to rumple to wavelengths ranging from 30–50 μm (Tolpygo and Clarke 2000) to about 300 μm (Pennefather and Boone 1995) upon thermal cycling to temperatures up to 1200°C in air. The amplitude of the rumpled surfaces in these experiments was up to 15 μm. Under very fast heating and cooling rates (1050°C to 300°C temperature change in less than a minute) along with mechanical loading of the superalloy substrate, the BCs did (Holmes and McClintock 1990, Zhang *et al.* 1999) or did not (Busso and McClintock 1993) show rumpling. Other effects related to thermal shock were observed in these experiments such as 'scalloping' (Holmes and McClintock 1990), i.e., large-scale spallation of the TGO and formation of highly elliptical voids (Busso and McClintock 1993). Under isothermal experiments at 1100°C

(Deb *et al*. 1987, Panat and Hsia 2004) and at 1150°C (Tolpygo and Clarke 2000), no rumpling was observed, while at 1175°C and at 1200°C BC was seen to rumple (Panat and Hsia 2004). Suo *et al*. (2003) found extensive void formation below the TGO after 300 h isothermal exposure in air at 1150°C.

To understand the BC rumpling phenomenon, one needs to address two important issues, *viz*, the driving force for rumpling and the mass transport mechanisms that lead to rumple formation. According to He *et al*. (2000) and Karlsson and Evans (2001), plastic ratcheting of the BC due to the thermal mismatch stresses in the developing TGO during thermal cycling can cause rumpling. Suo (1995), on the other hand, has suggested that the highly compressive growth stresses in the TGO (on the order of GPa) would provide the driving force necessary for the metal atoms to diffuse along the TGO–metal interface, leading to a wavy metal surface. In a recent model, Balint and Hutchinson (2003) have shown that the compressive stresses in the TGO along with the stresses in the BC can lead to rumpling under the conditions of the BC undergoing power-law creep (dislocation creep). The above models are generic to metal–oxide systems and require the existence of a highly stressed TGO for rumpling to occur. Tolpygo and Clarke (2000) have speculated that the rumpling in BC–superalloy systems occurs as a result of differential diffusion of various constituents such as Ni and Al, perpendicular to the BC surface. The model of Panat *et al*. (2003) is based on the assumption that the stresses in BC provide the necessary driving force for rumpling. A balance between the strain energy density at the BC surface and the BC surface energy would then determine the characteristic rumple wavelength. The mechanism they (Panat *et al*. 2003) proposed was the surface diffusion of BC atoms.

Thus, the possible deformation mechanisms of rumpling include: (1) cyclic plastic ratcheting of the BC driven by the stresses in the TGO; (2) dislocation creep in the BC driven by the stresses in the TGO and the BC; and (3) diffusive processes in the BC driven by the material concentration gradients in the BC cross-section, influenced by the stresses in the BC and/or in the TGO. The sources of the stresses in the TGO include its thermal mismatch with the BC (He *et al*. 2000, Tolpygo and Clarke 2000) and its own growth at high temperatures (Suo 1995), while those in the BC include its thermal mismatch with the superalloy substrate (Karlsson and Evans 2001, Watanabe *et al*. 2002, Panat *et al*. 2003), the phase transformation occurring in the BC at 650–700°C (Chen *et al*. 2003), or as a response to a highly stressed TGO. The diffusive processes contributing to the deformation in the BC, either near the BC surface or in the BC itself driven by BC stresses, include surface diffusion, bulk diffusion, grain boundary diffusion, and interdiffusion between the BC and the superalloy substrate.

The current experimental investigation stems from the desire to clarify the driving force and the kinetic processes governing the rumpling phenomenon in BC–superalloy systems in the absence of a ceramic topcoat. We carry out isothermal experiments at various temperatures up to 1200°C in vacuum on platinum aluminide and nickel aluminide BCs deposited on René N5, a Ni-based superalloy. The nickel aluminide BC is shown to form clear rumples in the absence of significant oxidation. The BC grains and the BC microstructure in this case were not seen to influence the rumpling behaviour. The platinum aluminide BC is shown to rumple at high temperatures, with the undulations correlated with the BC grains. It is shown that micron-scale mass transport due to diffusive processes in the BC driven by the BC stresses can result in the observed rumpling. These diffusive processes include grain

boundary diffusion, surface diffusion or bulk diffusion, or a combination of these processes.

§ 2. Experimental procedure

The superalloy substrate used in the present study was René N5, a Ni-based superalloy supplied by General Electric Aircraft Engines (Cincinnati, OH, USA). The BCs were deposited on the superalloy by Chromalloy Gas Turbine Corporation (Orangeburg, NY, USA). The platinum aluminide BC deposition process involved electroplating a Pt layer on the superalloy followed by a vacuum heat treatment and a vapour phase aluminisation. The nickel aluminide BC was deposited on the superalloy substrate by vapour phase aluminisation. The test samples were approximately 5 mm × 5 mm × 3–5 mm in dimension.

The nickel aluminide BCs were subjected to isothermal exposure at 1150°C, 1175°C and 1200°C. The surfaces of these BCs were in as-received condition or were polished using diamond paste to partially or completely remove the initial surface undulations. The platinum aluminide BC surfaces were polished down to 1 μm diamond paste and subjected to 1175°C and 1200°C. The amount of material removed during polishing is less than 10 μm from the top surface. Some platinum aluminide BC specimens with an as-deposited surface were also subjected to isothermal exposure at 1200°C. The holding times for the experiments were 25 h and 50 h. The holding time and temperature of exposure as well as the initial BC surface conditions were chosen to capture the important features of the behaviour of these coatings at high temperatures in vacuum.

A tube furnace (HTF55322A, Lindberg/Blue M, Asheville, NC, USA) along with a quartz tube carrying the BC–superalloy specimens was used for the experiments. The tube was connected to a roughing pump/diffusion pump assembly to produce a vacuum level up to 10^{-8} Torr at 1200°C. In some experiments, the vacuum level was seen to fall occasionally to about 10^{-6} Torr. The furnace provided a linear heating rate of about 22°C per minute for all the experiments. The samples were furnace cooled at the end of the hold time for each of the experiments. The specimen temperature was measured using a K-type thermocouple (Omega, Stamford, CT, USA) calibrated by an optical pyrometer (Pyrometer Instrument Company Inc., Northvale, NJ, USA). The specifications of the thermocouple indicate that the estimated error in the temperature measurements was less than ±0.75% when measured in degrees centigrade, i.e., less than ±7.5°C at a holding temperature of 1000°C. Some of the samples were cut and their cross-section polished successively down to 1 μm diamond paste to observe the microstructural changes. The samples were examined using profilometry, scanning electron microscopy (SEM), and the semi-quantitative elemental analysis tools of energy dispersive X-ray spectroscopy (EDX), X-ray photoelectron spectroscopy (XPS), and Augur electron spectroscopy (AES).

§ 3. Results

3.1. *Initial microstructure and composition*

Figure 1 shows representative SEM images of the cross-section and top views of the as-received nickel aluminide BC (figures 1(*a*) and (*c*)) and the platinum aluminide BC (figures 1(*b*) and (*d*)). The corresponding profilometer scans can be seen in figures 1(*e*) and (*f*), respectively. The composition of nickel aluminide BC is (wt%) 13.7Al–6Cr–7.8Co–bal Ni, while that of the platinum aluminide

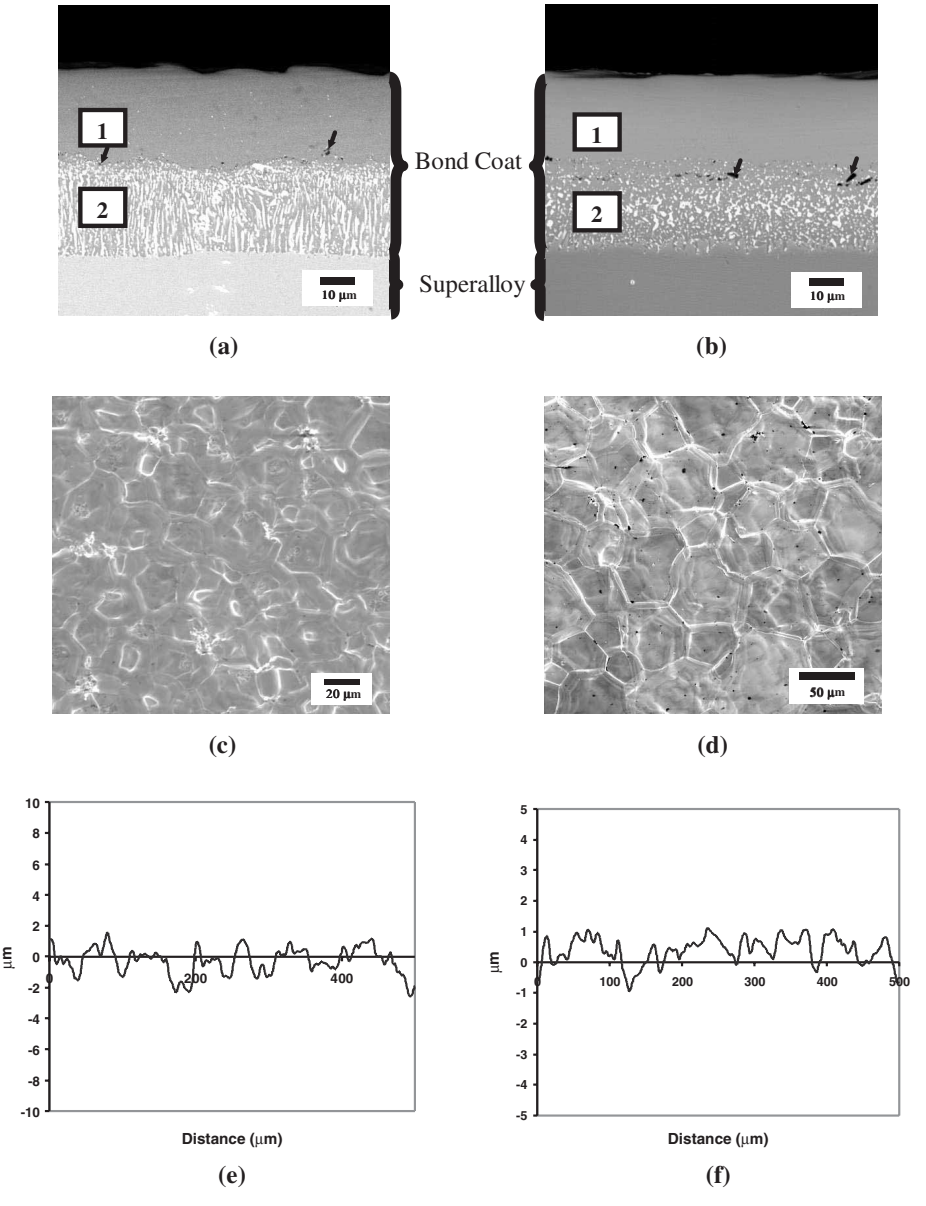

Figure 1. Cross-sectional SEM micrographs (with backscatter electrons) of (*a*) nickel aluminide BC and (*b*) platinum aluminide BC. Both BCs show an outer zone, '1', and an interdiffusion zone, '2'. Black arrows show alumina inclusions regularly placed between the two regions. (*c*) and (*d*) Top views of the nickel aluminide and the platinum aluminide BC, respectively. Ridges along the grain boundaries are clearly visible. (*e*) and (*f*) Profilometer scans of the nickel aluminide and platinum aluminide BC surfaces, respectively.

BC is (wt%) 17Al–7Cr–9Co–40Pt–bal Ni as determined by EDX analysis. Both BCs show a two-layered structure consisting of an outer zone (labelled '1') and an interdiffusion zone, or IDZ (labelled '2'). The IDZ of both BCs contains precipitates (bright regions in figures 1(*a*) and (*b*)) rich in refractory elements, *viz*, W,

Mo, and Ta. Alumina inclusions, shown by black arrows in figures 1(*a*) and (*b*), are irregularly placed at the border between region 1 and region 2. The BC compositions in the outer zones of the two BCs varied slightly in the direction perpendicular to the BC surface. For nickel aluminide BC, the Al content decreased from the top (about 18 wt%) to the IDZ (about 11 wt%), with a concomitant rise in the Co and Cr content. For the platinum aluminide BC, the Al content decreased from the top (about 22 wt%) to the IDZ (about 15 wt%), with a similar increase in the Co and Cr content. The nickel aluminide and the platinum aluminide BC grains can be seen in figures 1(*c*) and (*d*), respectively. The grain size for the nickel aluminide BC is about 20 μm while that for the platinum aluminide BC is about 30–50 μm. The composition of the René N5 superalloy (Walston *et al.* 1996) is (wt%) 7.5Co–7Cr–1.5Mo–6.5Ta–5W–3Re–6.2Al–0.15Hf–0.05C–0.004B–0.01Y–bal Ni.

3.2. *Isothermal exposure in vacuum: nickel aluminide BC*

Figure 2 shows the nickel aluminide BC surface (figures 2(*a*) and (*c*)) and the corresponding profilometer scan (figure 2(*b*)) after isothermal exposure in vacuum at 1200°C for 25 h. Clearly, the surface has developed rumples with a wavelength of 60–100 μm and an amplitude of 5–8 μm. This range of wavelengths and amplitude is comparable to that observed in the literature (Deb *et al.* 1987, Holmes and McClintock 2000, Tolpygo and Clarke 2000, Panat *et al.* 2003) during cycling and isothermal experiments on BCs in air. In figure 2(*c*), the BC grain boundaries are seen in addition to the BC rumples. Although a few BC grain boundaries were aligned along the rumple valleys, it is apparent that there is little correlation between the BC grains and the waviness. The difference in the periodicity of the rumples (figure 2(*b*)) and the BC grain size (figure 2(*c*)) confirms this conclusion. The rumpling seen in figure 2(*c*) has a local directionality, a feature also observed for platinum aluminide BCs under thermal cycling (Tolpygo and Clarke 2000, Panat and Hsia 2004). The reason for this phenomenon is not known at present, but it possibly happens because of local anisotropy in the BC material characteristics.

To estimate the thickness of the oxide layer developed over the BC, we use the method proposed by Strohmeier (1990) and Finnie *et al.* (2000). An XPS spectrum representing the Al 2p peak envelope of the BC surface is obtained as shown in figure 3. The binding energies of the peaks representing Al metal and Al oxide are sufficiently apart to obtain the individual areas under the peaks (figure 3). Since the TGO over the BC surfaces is an Al oxide, the areas computed under these peaks can be utilized to estimate the oxide layer thickness (Strohmeier 1990, Finnie *et al.* 2000). Although this method is used to obtain the thickness of Al oxide over pure Al metal, it can also be used for an *estimate* of oxide thickness over an Al alloy by assuming that the metals other than Al are replaced by Al. The ratio of the areas under the peaks representing the Al metal and the Al oxide is about 1/6.3 (from the curve-fit in figure 3). This gives an oxide thickness of about 1.7 nm (Finnie *et al.* 2000) or 2.3 nm (Strohmeier 1990). Thus, it is concluded that the oxide layer over the BC is only about a few nanometres thick, close to the native oxide thickness for Al (Saif *et al.* 2002).

Figure 4 shows an SEM micrograph (with backscatter electrons) of the cross-section of the rumpled sample in figure 2, revealing several interesting features formed after the thermal treatment in vacuum. The BC grain boundaries are revealed in the cross-section as the brighter regions seen due to chemical composition changes as indicated in the high-magnification micrograph of figure 4. Large bright regions

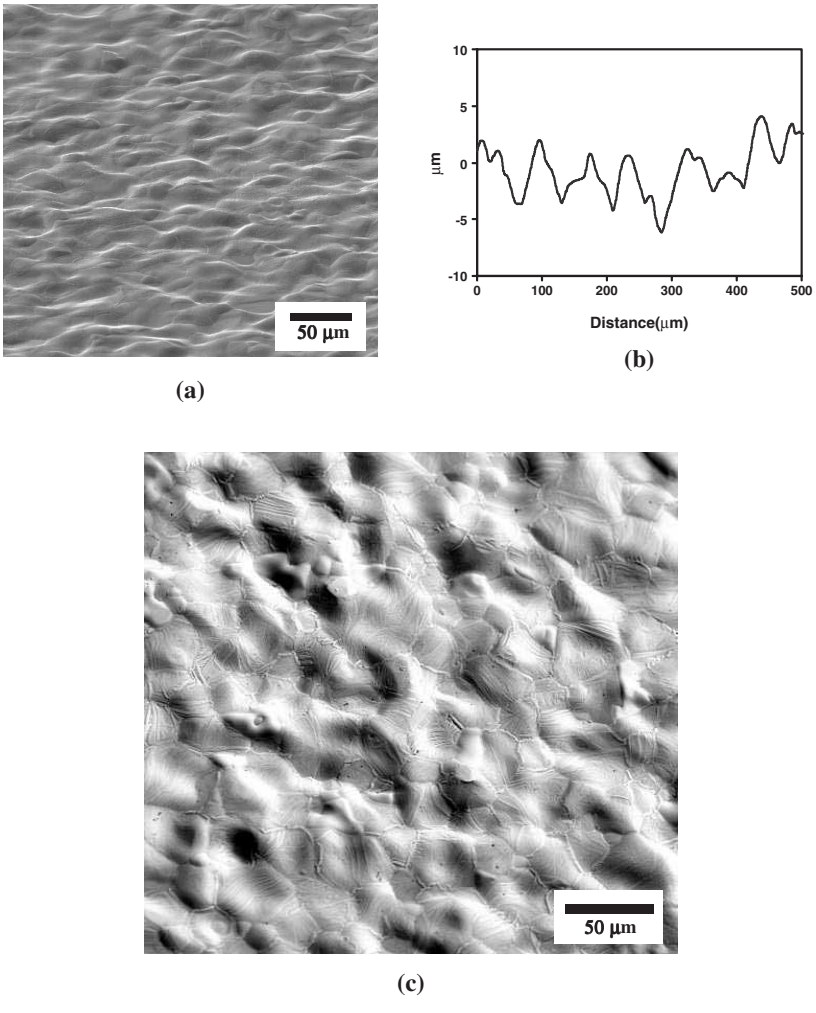

Figure 2. Nickel aluminide BC after 25 h isothermal exposure at 1200°C in vacuum. (*a*) SEM micrograph showing BC surface rumpling taken at a tilt of 30° with respect to the BC top surface; (*b*) the corresponding profilometer scan. (*c*) Top view of the same surface showing grains and rumpling. The BC grains have little correlation with rumple formation.

indicated by 'n' can also be seen along the grain boundaries where aluminium was depleted (about 5 wt% Al) when compared with the BC matrix (about 11 wt% Al). The composition of the grain boundaries was identical to that of these bright regions. The overall loss of Al in the BC in the absence of oxidation can be attributed to its diffusion to the superalloy at high temperatures (Tolpygo and Clarke 2000). Alumina inclusions (denoted by 'm') are seen as the dark regions in the higher-magnification micrograph of figure 4. These alumina inclusions were present before the isothermal exposure as shown in figure 1(*a*). The IDZ of the BC has developed random precipitates (denoted by 'p') rich in W, Mo and Ta. These precipitates, when compared with the as-deposited condition (figure 1(*a*)), have undergone considerable coarsening and agglomeration upon high-temperature

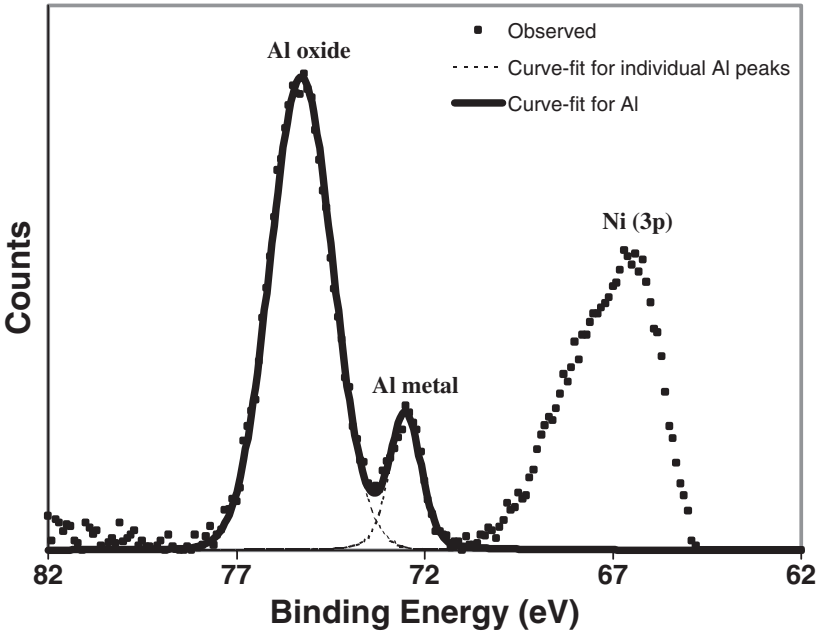

Figure 3. XPS spectrum of the BC surface showing the Al 2p peak envelope. The fitted curves for the individual peaks give the areas under the Al 2p peaks representing Al metal and Al oxide. The relative areas under the peaks of Al metal and Al oxide can be used to estimate the Al oxide layer thickness. An additional peak due to Ni 3p is also seen.

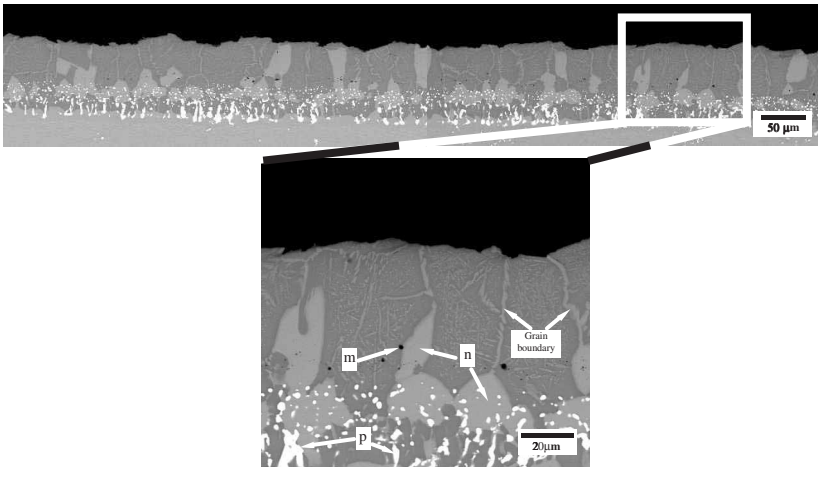

Figure 4. A representative SEM micrograph (with backscatter electrons) of the nickel aluminide BC cross-section showing the microstructure after 25 h isothermal exposure at 1200°C. The grain boundaries can be seen as brighter regions in the cross-section as indicated in the micrograph with higher magnification. Large bright regions indicated by 'n' are seen to have developed along the grain boundaries. Alumina inclusions denoted by 'm' are seen as the dark regions at the boundary of the outer and the inner region of the BC. These alumina inclusions were present before the isothermal exposure (figure 1(*a*)). Regions 'p' represent precipitates rich in W, Mo and Ta, also present before thermal cycling (figure 1(*a*)).

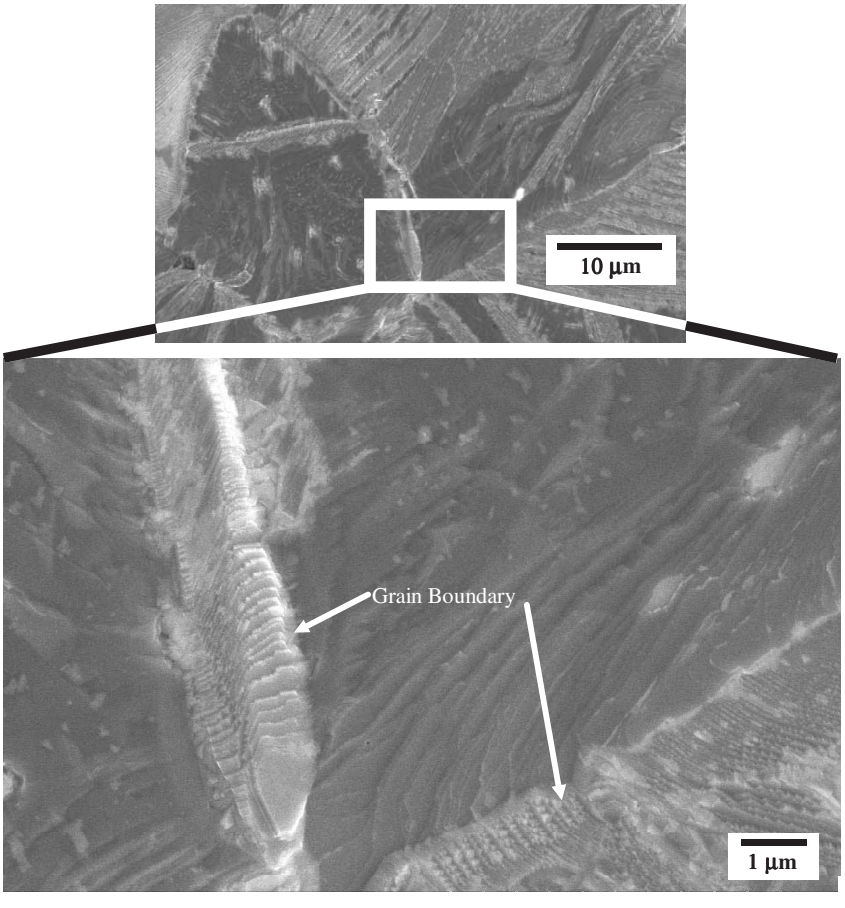

Figure 5. SEM micrographs showing faceting at the grain boundaries and in the grain interior of the nickel aluminide BC surface after 25 h isothermal exposure at 1200°C in vacuum.

exposure. The BC also shows a considerable increase in thickness when compared with the as-deposited condition in figure 1. The visibility of the BC grains in figure 2(*c*) is due to extensive faceting of the BC surface developed upon thermal treatment in vacuum as shown in figure 5. Figure 5 shows that the facets along the grain boundaries and the interior of grains have a periodicity of about 200–300 nm. Interestingly, the BC has developed a waviness of tens of micrometres, essentially unaffected by these smaller-scale features. Note that the directionality of these features was different for different BC grains.

To assess the effect of the initial surface roughness on waviness formation, a nickel aluminide BC sample was polished down to 1 μm diamond paste and subjected to isothermal exposure for 25 h at 1200°C in vacuum. Figures 6(*a*) and (*b*) show the initial surface of the BC and the corresponding profilometer scan. The initial BC surface undulations in figure 6(*b*) are about 30–40 nm in amplitude (peak to valley distance). After the isothermal exposure, the BC surface rumpled with an amplitude of about 4 μm, a two orders of magnitude increase as shown in figures 6(*c*) and (*d*). The inset in figure 6(*c*) shows the rumpling and the BC grains with no apparent correlation between the two, similar to the sample shown in figure 2.

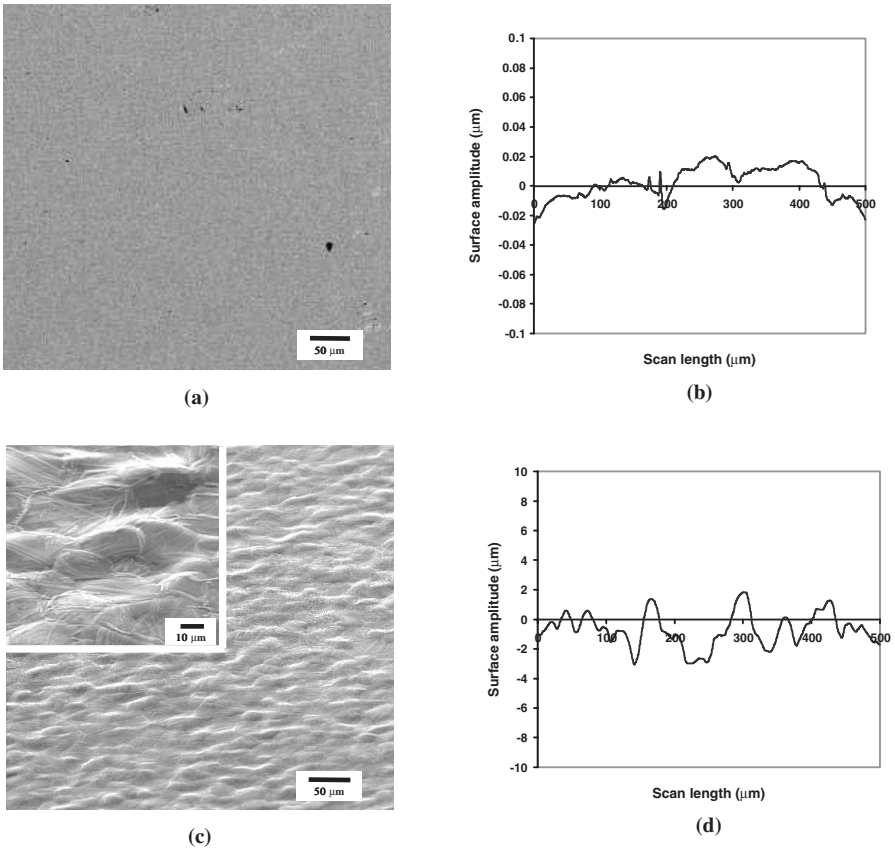

Figure 6. (*a*) and (*b*) SEM micrograph and the corresponding profilometer scan of the initial surface of a nickel aluminide BC. (*c*) SEM micrograph showing the rumpling of the same BC surface after 25 h at 1200°C in vacuum. (*d*) The profilometer scan of the surface shown in (*c*). The micrographs were taken at a tilt of 30° to the BC top surface.

The results of thermal exposure at 1175°C and 1150°C are shown in figure 7. Figure 7(*a*) shows the BC surface after 50 h thermal exposure at 1175°C. This surface topography is quite similar to that for the specimen exposed to 1200°C, as seen in figure 2(*b*). At this slightly lower temperature, however, some of the BC grain boundaries can be seen to correlate with the rumpling ridges. At 1150° after 25 h exposure, the BC surface shows no clear long-range rumpling, but small fluctuations correlated with the grain boundaries can be observed over the surface (figure 7(*b*)).

3.3. *Isothermal exposure in vacuum: platinum aluminide BC*

Figure 8 shows the surface morphology of a platinum aluminide BC before (figure 8(*a*)) and after (figures 8(*b*) and (*c*)) 25 h thermal exposure at 1200°C in vacuum. Clearly, upon isothermal exposure, the initial polished surface with fluctuations of about 20 nm in amplitude (figure 8(*a*)) developed a rumpled surface with an amplitude of fluctuation of about 5–7 μm (figures 8(*b*) and (*c*)). This two orders of magnitude increase in amplitude is similar to that for the nickel aluminide BC shown in figure 6. Unlike the nickel aluminide BC, however, the rumpling of the platinum aluminide BC was closely correlated with the BC grains; the grain boundaries being

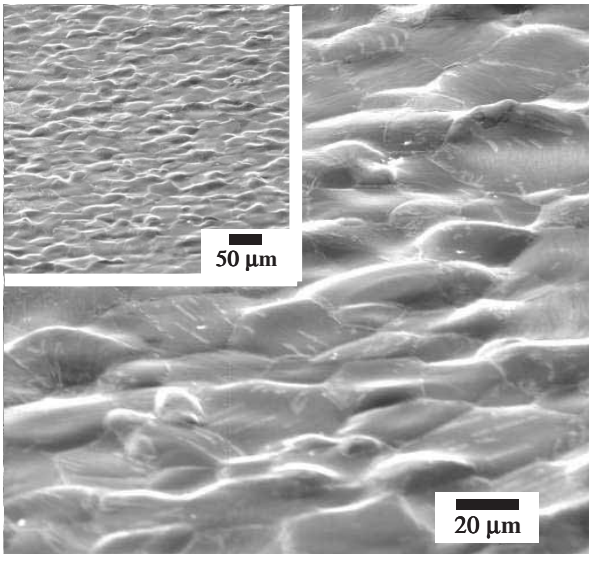

(a)

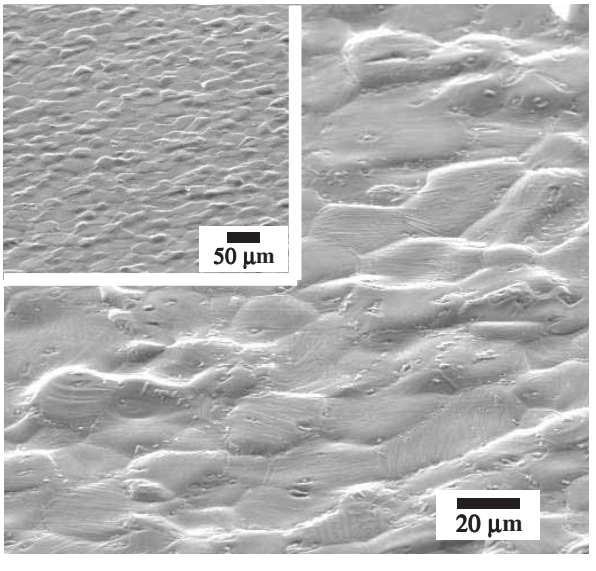

(b)

Figure 7. SEM micrograph showing the nickel aluminide BC (*a*) after 50 h exposure at 1175°C in vacuum, and (*b*) after 25 h exposure at 1150°C in vacuum. The micrographs were taken at a tilt of 30° (*a*) and 42° (*b*) to the BC top surface.

'depressed', while the grain interiors were 'elevated'. The grain interior and boundary structures can be seen in the high-resolution SEM micrographs of the same BC surface in figure 9. Extensive faceting developed over the BC grain surfaces and along the grain boundaries. Note that these facets have a periodicity of about 100–200 nm, similar to that for the rumpled nickel aluminide BC (figure 5).

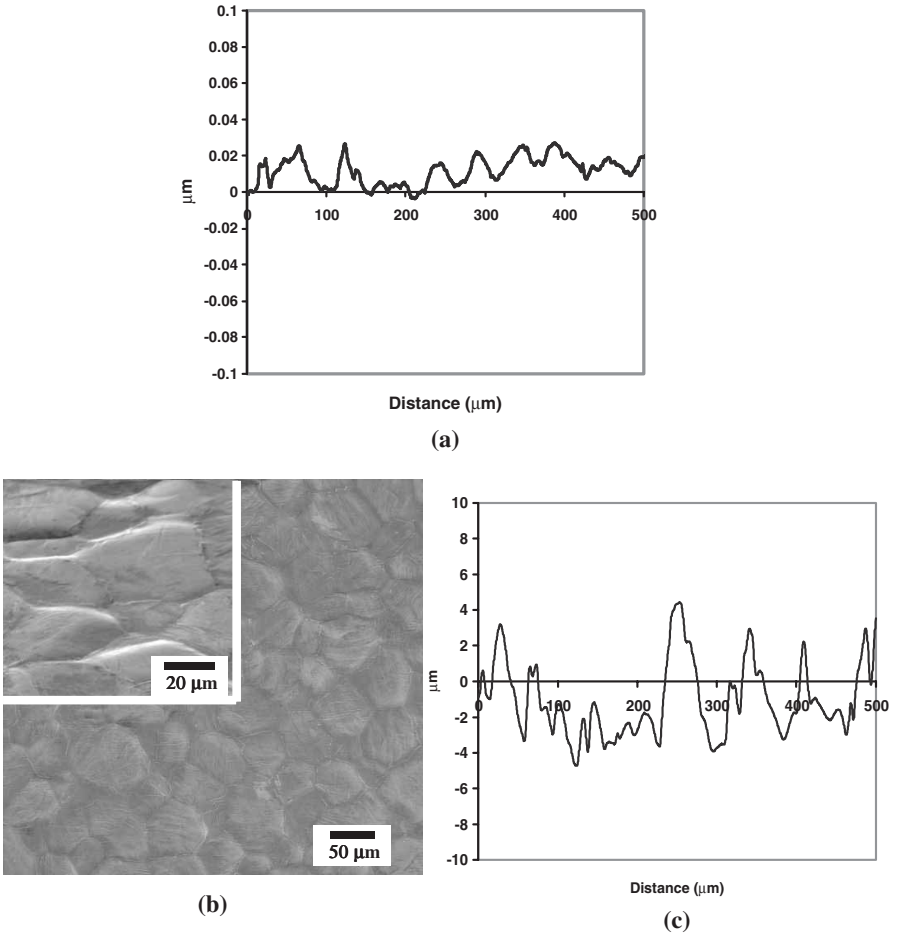

Figure 8. Platinum aluminide BC (*a*) profilometer scan before thermal treatment, (*b*) SEM micrograph after 25 h exposure at 1200°C in vacuum, and (*c*) the profilometer scan of the surface shown in (*b*). The high-magnification inset in (*b*) was taken at a tilt of 30° to the BC top surface.

The thickness of the oxide layer over the platinum aluminide BC could not be estimated using the XPS method (Strohmeier 1990, Finnie *et al.* 2000) due to the Al 2p peaks being overlapped by the Pt 4f peaks. We used AES to obtain the elemental composition as a function of depth over the platinum aluminide BC surface (figure 8(*b*)) as shown in figure 10 to measure the oxide thickness. Argon ions at 3 keV were used to sputter (remove) the surface material successively. The measurement was found to be repeatable on different platinum aluminide BC grain interiors. From figure 10, a significant signal attributed to Ni and Pt can be observed at a depth greater than about 2 nm. At the same time, the oxygen decreases with sputter depth, corresponding to the removal of the oxide. The error in the measurement is less than about ±2.5 nm, corresponding to the inelastic mean free path of Auger electrons before escaping a surface. Clearly, the oxide thickness for the platinum aluminide BC is less than 5 nm, comparable to that over the nickel aluminide BC. Further, figure 10 indicates that there is no Si contamination of the

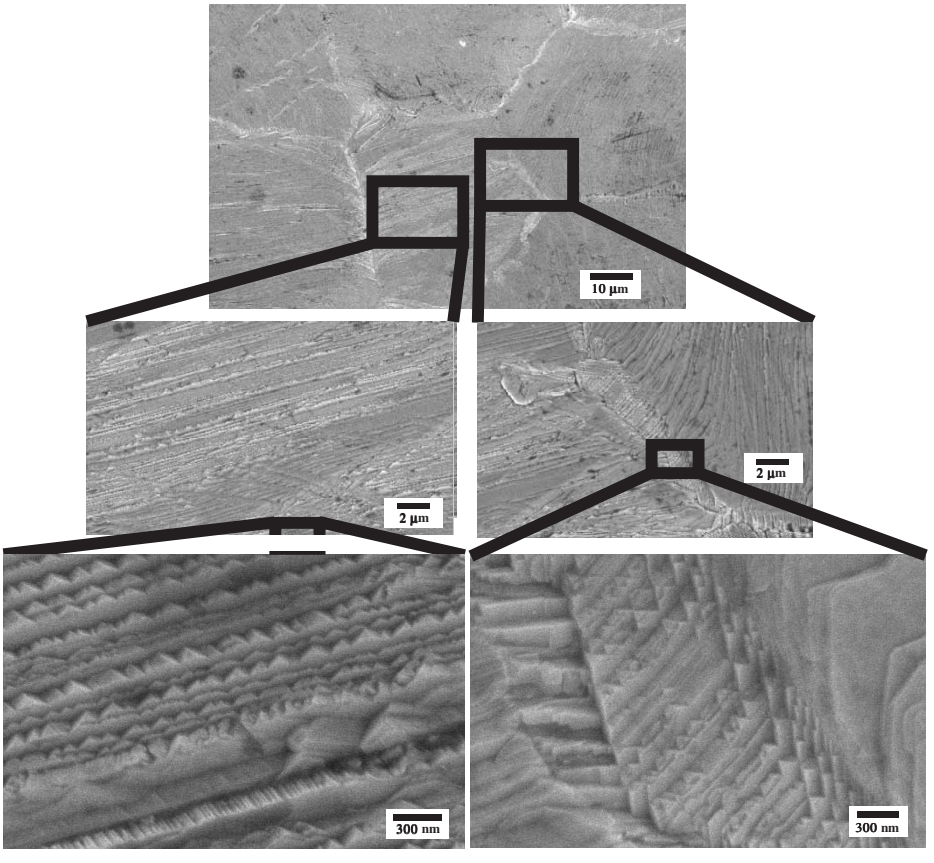

Figure 9. High-magnification SEM micrographs of the rumpled platinum aluminide BC shown in figure 8(*b*). Extensive facets developed over the grain surface and a *depressed* grain boundary (also showing facets) can be seen.

specimen surface, a phenomenon caused by possible evaporation of SiO_2 at high temperature and high vacuum.

Figure 11 shows a SEM micrograph (with backscatter electrons) of the cross-section of the rumpled sample in figure 8, revealing features quite similar to that for the nickel aluminide BC (figure 4). Large bright regions indicated by 'r' can also be seen where aluminium was depleted (about 7 wt% Al) when compared with the BC matrix (about 15 wt% Al). The overall loss of Al in the BC in the absence of TGO can again be attributed to its diffusion to the superalloy at high temperatures (Tolpygo and Clarke 2000). Unlike the nickel aluminide BC, the platinum aluminide BC grain boundaries were not revealed in the cross-section even with the contrast of the backscatter electrons. Alumina inclusions (denoted by 'q') are seen as the dark regions in the higher-magnification micrograph of figure 11. These alumina inclusions were present before the isothermal exposure, as shown in figure 1(*b*). An isolated void can be seen in the BC cross-section as shown by the black arrow in figure 11. The IDZ of the BC has developed precipitates (denoted by 's') rich in W, Mo and Ta. These precipitates, similar to the nickel aluminide BC (figure 4), have undergone considerable coarsening and agglomeration upon high-temperature exposure. The BC has also shown an increase in thickness when compared with

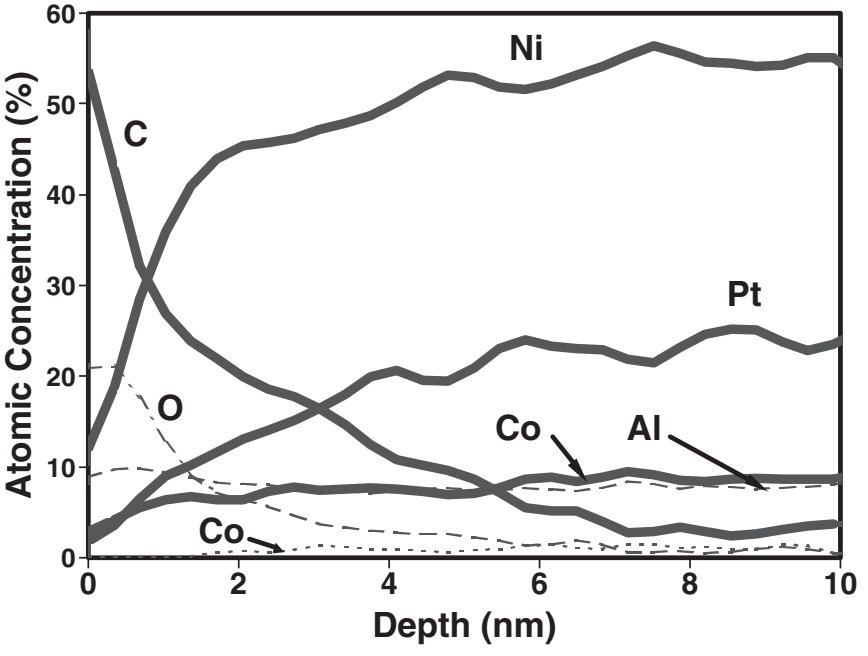

Figure 10. AES spectrum of the platinum aluminide BC surface shown in figure 8(*b*) as a function of sputter depth.

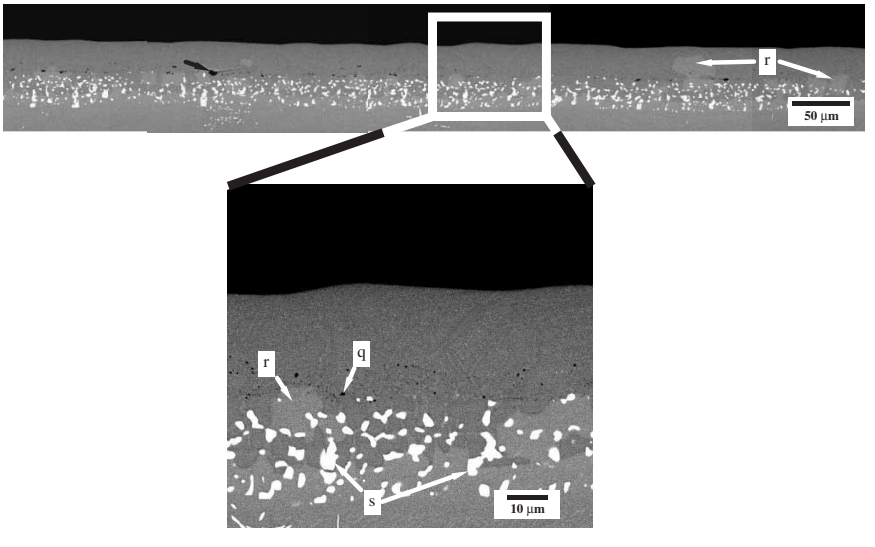

Figure 11. A representative SEM micrograph (with backscatter electrons) of the platinum aluminide BC cross-section showing the microstructure after 25 h isothermal exposure at 1200°C. Large bright regions (denoted by 'r') and alumina inclusions (denoted by 'q') are seen to have developed at the boundary between the outer and the inner regions. The alumina inclusions were present before the isothermal exposure (figure 1(*a*)). An isolated void is shown by the black arrow. Regions 's' represent precipitates rich in W, Mo and Ta that were also present before thermal cycling (figure 1(*a*)).

the as-deposited condition (figure 1(*b*)). The increase in the BC thickness and the coarsening of the refractory-rich precipitates upon high-temperature exposure for the two BCs (figures 4 and 11) has been observed during BC thermal cycling and isothermal exposure in air (Holmes and McClintock 1990, Busso and McClintock 1993, Tolpygo and Clarke 2000, Panat and Hsia 2004). Such a phenomenon is attributed to the diffusion of Ni from the superalloy to the BC at high temperature and the subsequent decrease of the solubility of refractory elements of the superalloy below the BC–substrate interface (Holmes and McClintock 1990, Busso and McClintock 1993).

In several observations at high temperatures (1150°C, 1175°C and 1200°C), clear rumpling could not be seen since the platinum aluminide BCs formed a non-uniform oxide layer over the surface, e.g. see figure 3.18 of Panat (2004). The platinum aluminide BC surface may develop isolated oxide sites and undulations with a periodicity of about 20 μm, smaller than that without any oxide formation. Note that, in ambient air, a continuous oxide layer is formed over the platinum aluminide BC at high temperatures (Tolpygo and Clarke 2000, Panat and Hsia 2004).

Table 1 summarizes all the experimental results presented in § 3.

§ 4. Discussion

The experimental results of the current study have shed light on clarifying the driving force for rumpling and identifying possible rumpling mechanisms. We have shown that mass transport leading to micron-scale deformations manifested in the form of rumpling can occur in BC–superalloy systems in the absence of a significant oxide layer. Also, the rumpling is shown to occur under isothermal conditions depending upon the temperature of testing. In the present section, we discuss the possible driving forces and the kinetics of rumpling.

4.1. *Driving force*

The prevailing view of many researchers states that the thin TGO under highly compressive stress provides the driving force for BC surface rumpling (Sou 1995,

Table 1. Summary of experiments.

Testing condition	Initial surface	Nickel aluminide BC	Platinum aluminide BC
1200°C 25 h	Polished	Surface rumpled with little or no correlation with BC grain structure	Surface rumpled with fluctuations correlated with BC grain structure
1200°C 25 h	As deposited	Surface rumpled with little or no correlation with BC grain structure	No observations due to non-uniform oxide formation
1175°C 50 h	Partially polished	Surface rumpled with some correllation to BC grain structure	Same as above
1150°C 25 h	Polished	Surface fluctuations correlated with BC grain structure	Same as above

He *et al.* 2000, Karlsson and Evans 2001, Balint and Hutchinson 2003) since such a thin layer has a tendency to buckle. In the present study, we demonstrate that rumpling occurred in the BC–superalloy systems even when the oxide layer over the BC was of insignificant thickness (e.g. figures 2 and 8). Clearly, this native oxide (a few nanometres thick) should not be the cause of the BC rumpling. This leaves the possibility of the concentration gradient of various elements in the BC (Tolpygo and Clarke 2000), or the stresses in the BC (Panat *et al.* 2003) as the possible driving force for rumpling. Figure 4 shows that the periodicity of the refractory-rich precipitates (indicated by 'p') does not match that of the rumples, neither do the aluminium-depleted zones that are irregularly placed, as shown in figure 4 (denoted by 'n'). Similarly, the aluminium-depleted zones and the refractory-rich regions of the platinum aluminide BC cross-section (figure 11) do not show a periodicity corresponding to the platinum aluminide surface undulations (figure 8). Furthermore, we did not observe any void formation in the nickel aluminide BCs upon isothermal exposure. The isolated voids formed in the platinum aluminide BC did not correspond to the rumples. It is clear that the material concentration changes in the BC cross-section show a poor correlation with the BC rumples. A similar conclusion was drawn concerning the role of the microstructure in inducing BC surface instabilities for the platinum aluminide BC–superalloy system both in the presence (Mumm *et al.* 2001) and the absence (Panat and Hsia 2004) of the ceramic topcoat in air.

This leaves us with the only viable alternative, i.e., *the stresses in the BC alone are capable of inducing BC rumpling* in nickel aluminide and platinum aluminide BC–superalloy systems under the current testing conditions. The origin of the BC stresses are believed to be the thermal mismatch between the BC material and the substrate, and possibly phase transformation (Karlsson and Evans 2001, Watanabe *et al.* 2002, Chen *et al.* 2003, Panat *et al.* 2003). Therefore, the magnitude of this driving force depends on how far the testing temperature is from the BC deposition temperature (Panat and Hsia 2004, Panat *et al.* 2004). Under different testing conditions, e.g. in air, the formation of TGO may potentially influence the rumpling behaviour. However, the present study shows that the characteristic wavelengths and the amplitudes of rumpled BC surfaces tested in vacuum are comparable to those tested in air (Deb *et al.* 1987, Tolpygo and Clarke 2000, Panat and Hsia 2004).

4.2. *Governing kinetics*

The fact that rumpling can occur under isothermal conditions indicates that cyclic plasticity, i.e. ratcheting of the BC (He *et al.* 2000), is not necessarily the dominant mechanism for rumpling. Although the exact role of the BC ratcheting on BC rumpling under other testing conditions is not known, it is likely to play a secondary role during rumpling even under thermal cycling (Panat and Hsia 2004). Further, the material concentration changes in the BC cross-section have a poor correlation with the rumples, indicating that differential diffusion of different constituents in the BC (Tolpygo and Clarke 2000) would not govern the kinetics of the rumpling seen in the current study. The recently suggested creep mechanism of Balint and Hutchinson (2003) is a plausible mass transport mechanism for BC surface rumpling. The small-scale faceting seen in figure 5 seems to lend support to such a dislocation creep mechanism during BC rumpling. However, such small-scale features with submicron dimensions do not correlate with the long wavelength of the rumpled surface as demonstrated in figure 2. Nevertheless, BC stress-induced creep deformation may potentially contribute to the rumpling process.

Other kinetic processes include diffusive mechanisms such as surface diffusion, volume diffusion, and grain boundary diffusion. The BC stress-driven surface diffusion model of Panat *et al*. (2003) can explain several experimental results of the nickel aluminide BC rumpling in the current study. Figures 2 and 6 show that the rumpling phenomenon is relatively insensitive to the initial surface fluctuations as predicted by the model (Panat *et al*. 2003). Further, this model predicts that rumpling under isothermal conditions in the absence of any oxide layer can occur, as observed in the current study. It is noted, however, that the model of Panat *et al*. (2003) only takes into account the surface diffusion mechanism, and does not take into account other diffusive mechanisms such as volume diffusion through the BC bulk and grain boundary diffusion (Mullins 1963, Shewmon 1989, Thouless 1993). New modelling efforts are being pursued to take into account all significant diffusive processes in the BCs to predict the rumpling behaviour (Panat *et al*. 2004). The fact that the rumpling is correlated with the grain structures in platinum aluminide BC points to the possibility that grain boundaries are an active diffusion path during rumpling. The difference in the dominant paths of diffusion in the case of the nickel aluminide and the platinum aluminide BCs is not currently known. It is conceivable that competition between grain boundary diffusion and the BC volume diffusion exists, and its outcome depends upon the testing temperature (Shewmon 1989). This competition arises due to the lower activation energy of grain boundary diffusion compared with that of volume diffusion. At moderately high temperatures, grain boundary diffusion forms the high diffusivity path. But as temperature increases, volume diffusion becomes dominant over grain boundary diffusion. Thus, a combination of BC volume diffusion and surface diffusion would decide the rumpling process at higher temperatures while, at lower temperatures, grain boundary diffusion should be observed. Qualitatively, we see that, at 1200°C, the BC surface undulations are not related to the grain structure (figure 2). But at 1175°C and at 1150°C an increased correlation between the two is seen (figure 7(*b*) and (*d*)). Unfortunately, the grain boundary diffusivity has not been measured in BC–superalloy systems. Further, we do not have quantitative information on the effect of grain size on rumpling behaviour, which we suspect would also depend on the testing temperature and thus the dominant diffusive mechanisms. To fully identify the dominant mechanism(s), a study aimed at measuring various diffusion constants in BC–superalloy systems at different temperatures needs to be carried out.

The processes leading to rumpling in the case of platinum aluminide BC shown in figure 8 could be a combination of surface and grain boundary diffusion. Such a process has been modelled by Thouless (1993) for an array of grains under a remote stress. His analysis shows that a combination of grain boundary diffusion and surface diffusion would give rise to surface morphologies similar to those seen in figures 8 and 9. Again, for any comparison, the diffusivity of platinum aluminide BC along various diffusion paths needs to be measured at various temperatures.

The results presented in the current study have important implications for the TBC failure process. Our main objective here is to identify the role of the BC stresses and the diffusive processes in TBC failure. These stresses appear to be important in the evolution of TBC systems during high-temperature exposure. The magnitude of the BC stress at different temperatures can be estimated by evaluating the thermal expansion coefficients (CTE) of the BCs and the substrate. The CTEs of platinum aluminide BC, nickel aluminide BC, and René N5 superalloy substrate are reported

to be about $15.5 \times 10^{-6\circ}C^{-1}$, $16 \times 10^{-6\circ}C^{-1}$, and $14 \times 10^{-6\circ}C^{-1}$ (Watanabe *et al.* 2002, Chen *et al.* 2003). Assuming that the BC is stress-free at the aluminisation temperature of about 1050°C, the stress in the BC can thus be estimated to be about 45 MPa in nickel aluminide BC and 35 MPa in platinum aluminide BC at 1200°C (Panat 2004). Such stress levels, although rather low, are comparable to the yield strength of the BC material at that temperature (Pan *et al.* 2003), and are sufficient to induce surface rumpling by combined surface and bulk diffusion (Panat and Hsia 2004).

Different diffusive processes in the BC could lead to surface rumpling of several micrometres in amplitude, which can contribute to debonding between the BC and the ceramic topcoat in a TBC system, leading to TBC failure. Although the constraints in real TBC systems due to the ceramic layer and the TGO may change the diffusion kinetics, these diffusive processes may still be important in inducing interface instability, especially at high temperatures and over prolonged periods of time. Tailoring the BC materials to maximize resistance to diffusion can potentially minimize BC deformation and prolong the life of TBC systems.

§ 5. Conclusion

In the present work, isothermal experiments were carried out on nickel aluminide and platinum aluminide BC–superalloy systems in vacuum. The results show that rumpling can occur under isothermal conditions in the absence of a significant oxide layer. The material concentration gradient in the BC cross-section does not show a correlation with the rumples. For nickel aluminide BC, the grain structure does not influence the rumpling behaviour at high testing temperatures. As the isothermal exposure temperature decreases, the BC grain boundaries increasingly influence the rumpling behaviour. For platinum aluminide BC, the rumples are correlated with the BC grains at the highest temperature of testing. Rumpling wavelength and amplitude are relatively insensitive to initial BC surface fluctuations in both BC material systems. Further, significant initial flaws are not needed for rumpling to occur. It is concluded that, in the absence of a significant oxide layer, the driving force for rumpling formation is likely to be the thermal mismatch stress in the BC. Possible kinetics that govern the rumpling process in the present study include a combination of diffusive processes such as surface, bulk and grain boundary diffusion. These findings have significant implications for the study of TBC reliability, since the diffusive processes in the BC driven by the BC stresses can potentially play a significant role in TBC failure.

Acknowledgements

This work is supported by a Critical Research Initiative program at the University of Illinois at Urbana-Champaign (UIUC). One of the authors (R.P.) would like to thank the Fellowships Office at UIUC for their support through a Dissertation Completion Fellowship. Thanks go to Dr. Ram Darolia of General Electric for providing the superalloys, and to Paul Lawton, Stacy Fang, and Anthony Collucci of Chromally, NY, USA for coating the superalloys with the bond coat. We are thankful to Dr. Nancy Fennegan at UIUC for the AES work. The SEM, XRD, AES and profilometry was carried out at the Center for Microanalysis of Materials, Frederick Seitz Materials Research Laboratory, UIUC, which is partially supported by the U.S. Department of Energy under

grant DEFG02-91-ER45439. The authors would like to acknowledge helpful discussions with Professor David Cahill, Dr. Rick Haasch and Dr. Ming Liu at UIUC.

References

Ali, M. S., Song, S., and Xiao, P., 2002, *J. Mater. Sci.*, **37**, 2097.

Ambrico, J. M., Begley, M., and Jordan, E. H., 2001, *Acta mater.*, **49**, 1577.

Balint, D. S., and Hutchinson, J. W., 2003, *Acta mater.*, **51**, 3965.

Bartlett, A. H., and Maschio, R. D., 1995, *J. Am. Ceram. Soc.*, **78**, 1018.

Bartsch, M., Baufeld, B., and Fuller, E. R. J., 2003, *Ceram. Engng; Sci. Proc.*, **16**, 497.

Bartsch, M., Marci, G., Mull, K., and Sick, C., 2001, *Int. J. Mater. Prod. Technol.*, **16**, 248.

Baufeld, B., and Barstch, M., 2003, *Fifth International Conference on Low Cycle Fatigue, Berlin, Germany*, edited by P. D. Portella, H. Sehitoglu and K. Hatanaka (Federation of European Materials Societies) (to be published).

Baufeld, B., Tzimas, E., Mullejans, H., Peteves, S., Bressers, J., and Stamm, W., 2001, *Mater. Sci. Engng.* A, **315**, 231.

Bose, S., and Demasi-Marcin, J., 1997, *J. Therm. Spray Technol.*, **6**, 99.

Bouhanek, K., Adesanya, O. A., Stott, F. H., Skeldon, P., Lees, D. G., and Wood, G. C., 2000, *Mater. high Temp.*, **2**, 185.

Busso, E. P., Lin, J., Sakurai, S., and Nakayama, M., 2001, *Acta mater.*, **49**, 1515.

Busso, E. P., and McClintock, F. A., 1993, *Mater. Sci. Engng.* A, **161**, 165.

Chen, M. W., Ott, R. T., Hufnagel, T. C., Wright, P. K., and Hemker, K. J., 2003, *Surf. Coat. Technol.*, **163/164**, 25.

Clarke, D. R., and Shillington, E. A. G., 1999, *Acta mater.*, **47**, 1297.

Deb, P., Boone, D. H., and Manley, T. F. I., 1987, *J. vac. Sci. Technol.*, **5**, 3366.

Evans, A. G., Mumm, D. R., Hutchinson, J. W., Meier, G. H., and Pettit, F. S., 2001, *Prog. Mater. Sci.*, **46**, 505.

Finnie, K. R., Haasch, R., and Nuzzo, R. G., 2000, *Langmuir*, **16**, 6968.

Goward, G. W., 1998, *Surf. Coat. Technol.*, **108/109**, 73.

He, M. Y., Evans, A. G., and Hutchinson, J. W., 2000, *Acta mater.*, **48**, 2593.

Holmes, J. W., and McClintock, F. A., 1990, *Metall. Trans.*, **21A**, 1209.

Ibegazene-Ouali, F., Mervel, R., Rio, C., and Renollet, Y., 2000, *Mater. high Temp.*, **17**, 205.

Karlsson, A. M., and Evans, A. G., 2001, *Acta mater.*, **49**, 1793.

Kim, G. M., Yanar, N. M., Hewitt, E. N., Pettit, F. S., and Meier, G. H., 2002, *Scripta mater.*, **46**, 489.

McDonald, G., and Hendricks, R. C., 1980, *Thin Solid Films*, **73**, 491.

Meier, S. M., and Gupta, D. K., 1994, *J. Engng. Gas Turbine Power*, **116**, 250.

Miller, R. A., 1987, *Surf. Coat. Technol.*, **30**, 1.

Miller, R. A., and Lowell, C. E., 1982, *Thin Solid Films*, **95**, 265.

Mullins, W. W., 1963, *Metal Surfaces*, edited by W. D. Robertson and N. A. Gjostein (Metals Park, OH: American Society for Metals), pp. 17–66.

Mumm, D. R., Evans, A. G., and Spitsberg, I. T., 2001, *Acta mater.*, **49**, 2329.

Padture, N. P., Gell, M., and Jordan, E. H., 2002, *Science*, **296**, 280.

Pan, D., Chen, M. W., Wright, P. K., and Hemker, K. J., 2003, *Acta mater.*, **51**, 2205.

Panat, R. P., 2004 *On the Rumpling Instability in Thermal Barrier Systems*, PhD Thesis, University of Illinois at Urbana-Champaign, Urbana, IL, USA.

Panat, R. P., and Hsia, K. J., 2004, *Proc. R. Soc. London, Ser.* A, **460**, 1957.

Panat, R. P., Hsia, K. J., and Cahill, D. G., 2004, *J. appl. Phys.* (accepted).

Panat, R. P., Zhang, S., and Hsia, K. J., 2003, *Acta mater.*, **51**, 239.

Pennefather, R. C., and Boone, D. H., 1995, *Surf. Coat. Technol.*, **76/77**, 47.

Ruud, J. A., Bartz, A., Borom, M. P., and Johnson, C. A., 2001, *J. Am. Ceram. Soc.*, **84**, 1545.

Saif, M. T. A., Zhang, S., Haque, A., and Hsia, K. J., 2002, *Acta mater.*, **50**, 2779.

Schulz, U., Leyens, C., Fritscher, K., Peters, M., Saruhan-Brings, B., Lavigne, O., Dorvaux, J., Poulain, M., Mevrel, R., and Calez, M., 2003, *Aero. Sci. Technol.*, **7**, 73.

Schulz, U., Menzebach, M., Leyens, C., and Yang, Y. Q., 2001, *Surf. Coat. Technol.*, **146/147**, 117.
Sheffler, K. D., and Gupta, D. K., 1988, *J. Engng. Gas Turbine Power*, **110**, 605.
Shewmon, P. G., 1989, *Diffusion in Solids*, 2nd edn (Warrendale, PA: The Minerals, Metals & Materials Society).
Stiger, M. J., Yanar, N. M., Topping, M. G., Pettit, F. S., and Meier, G. H., 1999, *Z. Metallk.*, **90**, 1069.
Strangman, T. E., 1985, *Thin Solid Films*, **127**, 93.
Strohmeier, B., 1990, *Surf. Interface Anal.*, **15**, 51.
Suo, Z., 1995, *J. Mech. Phys. Solids*, **43**, 829.
Suo, Z., Kubair, D., Evans, A. G., Clarke, D. R., and Tolpygo, V., 2003, *Acta mater.*, **51**, 959.
Thouless, M. D., 1993, *Acta metall. mater.*, **41**, 1057.
Tolpygo, V. K., and Clarke, D. R., 2000, *Acta mater.*, **48**, 3283; 2001, *Elevated Temperature Coatings: Science & Technology IV*, edited by N. B. Dahotre, J. M. Hampikian and J. E. Morral (Warrendale, PA: The Minerals, Metals & Materials Society), pp. 94.
Tolpygo, V. K., Clarke, D. R., and Murphy, K. S., 2001, *Surf. Coat. Technol.*, **146/147**, 124.
Vaidyanathan, K., Gell, M., and Jordan, E., 2000, *Surf. Coat. Technol.*, **133/134**, 28.
Walston, W. S., O'Hara, K. S., Ross, E. W., Pollock, T. M., and Murphy, W. H., 1996, *Proceedings of the Superalloys Symposium*, edited by R. D. Kissinger, D. J. Deye, D. L. Anton, A. D. Cetel, M. V. Nathal, T. M. Pollock and D. A. Woodford (Warrendale, PA: The Minerals, Metals & Materials Society), pp. 27–33.
Watanabe, M., Mumm, D. R., Chiras, S., and Evans, A. G., 2002, *Scripta mater.*, **46**, 67.
Wright, P. K., 1998, *Mater. Sci. Engng.* A, **245**, 191.
Wright, P. K., and Evans, A. G., 1999, *Curr. Opin. Solid St. Mater. Sci.*, **4**, 255.
Wu, B. C., Chang, E., Chang, S. F., and Chao, C. H., 1989, *Thin Solid Films*, **172**, 185.
Zhang, Y. H., Withers, P. J., Fox, M. D., and Knowles, D. M., 1999, *Mater. Sci. Technol.*, **15**, 1031.